

## Activated carbon synthesis using Moroccan dates stones as precursor and application for wastewater treatment

I. EL Aboudi<sup>a,\*</sup>, H. Annab<sup>a,b</sup>, A. Mdarhri<sup>a</sup>, M. Amjoud<sup>a</sup>, L. Servant<sup>c</sup>

<sup>a</sup>Laboratory of Condensed Matter and Nanostructures (LCMN), Faculty of Sciences and Technology University of Guèliz, BP 549, Av Abdelkarim Elkhatabi, 40000 Marrakech, Morocco

<sup>b</sup>Laboratory of Chemistry and Environment (LCME), Faculty of Sciences and Technology Guèliz, University of BP 549, Av Abdelkarim Elkhatabi, 40000, Marrakech, Morocco

<sup>c</sup>University of Bordeaux, Institute of Molecular Sciences, Group of Molecular Spectroscopy, UMR5255, BP 351, Cours de la Libération, Talence, France

Received 04 Jun 2016,  
Revised 10 Jul 2016,  
Accepted 15 Jul 2016

### Keywords

- ✓ Date stones,
- ✓ Chemical activation,
- ✓ Activated carbon,
- ✓ Water treatment,
- ✓ Adsorption,
- ✓ Dyes

[i.elaboudi@uca.ma](mailto:i.elaboudi@uca.ma)

### Abstract

Owing to its high carbon content, we report in this paper the use of Moroccan date stones (DS) as a potential precursor for the production of porous activated carbons (AC) which could be used in water treatment applications. In this experimental investigation, DS were chemically activated by using various impregnation ratio  $\chi_p$ , defined as the weight ratio of impregnant (phosphoric acid) to precursor, followed by heat treatment at 450°C under nitrogen stream for two hours. Fourier Transform Infrared spectroscopy was used to investigate the chemical structure of DS based activated carbon (AC). Furthermore, the textural properties of AC were characterised using scanning electron microscopy and nitrogen adsorption-desorption isotherms. Structural characteristics including surface area; pores size distribution and pores total volume estimations are reported. The largest specific surface area ( $\approx 766 \text{ m}^2/\text{g}$ ) associated to a high microporous volume ( $0.704 \text{ cm}^3/\text{g}$ ) were obtained when DS were activated with an impregnation ratio being equal to  $\chi_p = 2$ . This highly porous AC was used in a model batch adsorption experiment involving an aqueous solution of methylene bleu (MB) and a maximum adsorption capacity was found to reach 21mg/g using a Freundlich adsorption model. This result suggests that dates stones derived activated carbon could be used as efficient adsorbent to remove hazardous materials from water with a high pollutant uptake capacity.

### 1. Introduction

In the 21th century, the world is more and more interested in the protection of the environment from the solid waste induced by the various human activities and surge of industrialization. The common and traditional solid waste disposal routes such as incineration, or composting and land application are easy and low cost but are not sustainable techniques due to lack of material recovery strategy and recycling approaches [1,2]. Hence, solid wastes like agriculture by-products that are rich in nitrogen, phosphorous and other organic components were used as additives in fertilizers [3]. Other options applied to solid-waste treatment were also employed, they include thickening, dehydration, drying and biological treatment [1,2,4]. However, these post-treatment methods raise the cost of recycling [5]. Therefore, it is important to produce a high profitable recycled material.

Most of emerging, ecological and low cost R&D techniques have been put into transforming agriculture by-products into activated carbon phases that could be used as adsorbent in wastewater treatment [6,7]. This type of material is known by its high adsorption capacity of different pollutants. Date stones are considered as one of the best precursor candidate among the agricultural by-products. Indeed, it is abundant in the south of Morocco where dates-fruit annual production is estimated to be 100,000 tons [6] placing the country at the 8th rank in production in the world. Dates stones are rich in carbohydrates. They are composed of 42% of cellulose, 18% of hemicellulose, 11% of lignin, 25% of sugar and 4% of ash [6]. Thus it promotes to use DS as precursor for activated carbon preparation. The adsorption efficiency of the activated carbon based DS depends on its porous

structure and on functional groups distributed over its surface. Both characteristics could be adapted by controlling the activation conditions, such as the method of activation: either physical or chemical ways, the choice of the activating agent, the impregnation ratio, the temperature and time of pyrolysis [1,2,4]. In physical activation process, the carbonaceous matter is pyrolyzed under a stream of mild oxidizing gas such, nitrogen or carbon dioxide. In chemical activation process, the precursor is impregnated with a dehydrating agent, such as phosphoric acid, zinc chloride, potassium hydroxide or potassium chloride. Then, the soaked matter is activated at high temperature under inert gas stream for more than 2 hours [8]. In most reported cases [1,2,8], chemical activation is preferred because the physical method has many drawbacks. It requires high pyrolysis temperature, longer time of heat treatment and produces low carbon yield. Conversely, chemical activation results in a high porous carbon with a lower energy cost. It has been widely used by many researchers for the preparation of activated carbons from different agricultural wastes using various chemical reagents, such as coconut shell combined to  $H_2SO_4$  [9], jatropha hull combined to  $ZnCl_2$  [10], and olive pomace combined to  $KOH$  [11]. Few studies involve the use of date stones based activated carbon in wastewater treatment [12-14] and vast disparities in results (specific surface, pore size distribution, the nature of functional groups on AC surface...etc) were observed if the operating conditions were not strictly controlled when considering water washing of impregnated date stones before or after pyrolysis and chemical composition of the precursor [1].

This work is devoted to prepare by chemical activation route highly porous activated carbon materials using Moroccan date stones as precursor. At the first step, the effect of phosphoric acid impregnation ratio on the resulting texture of AC is examined in order to enhance its synthesis efficiency with suitable operating conditions. The as-synthesized AC samples were then probed by FTIR spectroscopy and the chemical transformation of date stones induced by activation was highlighted. Additional structural characterizations including specific surface area, pore volume and pore size distribution were also performed using scanning electron microscopy and  $N_2$  adsorption-desorption isotherms. Finally, the highest porous prepared AC sample was investigated in a model batch adsorption experiment of methylene blue from an aqueous solution.

## 2. Materials and methods

### 2.1 Date stones pre-treatment

“Bu-Shamî” date stones variety was collected from the region of Zagora which is situated in the south of Morocco. They were used as a precursor for the production of activated carbons via chemical activation and by using phosphoric acid as an impregnating agent. Prior to activation, the raw material was washed with distilled water to remove physical impurities. After that, it was air-dried overnight at  $110^\circ C$  before ongoing milling and sieving operations. Precursor particles having the size range of 0.5 to 1.5mm were selected for preparing activated carbon samples.

### 2.2 Chemical activation

In this subsection, the chemical activation route adopted in this study is described as follows. 20 g of pre-treated DS were added to phosphoric acid (weight concentration 60%) with different impregnation ratio (1; 1.5; and 2). The impregnation was carried out at  $85^\circ C$  during 2 hours in a stirred Pyrex reactor equipped with a reflux condenser. Stirring improves acid diffusion in the bulk of the DS particles. After the impregnation, the mixture was heated up to  $100^\circ C$  in order to evaporate the excess of diluted acid, and to accelerate the kinetics of the reaction between the precursor and the acid. The resulting mixture was filtered and dried in an oven at  $105^\circ C$  during 24h. Pyrolysis of the impregnated DS was then carried out by using a silica tube reactor (2,5 cm x 10 cm) where nitrogen stream flows at 100ml/min flow-rate. The heat treatment was performed by placing the reactor in a horizontal tubular furnace equipped by heating controller GEFTRAN 1600PM. Temperature was raised from the ambient to  $450^\circ C$  with a  $10^\circ C/min$  heating rate. Finally, the temperature was kept at  $450^\circ C$  during two hours. At the end of the pyrolysis step, heating was turned off and samples were cooled to ambient temperature under nitrogen stream with  $2^\circ C/min$  cooling rate. In order to eliminate the residual acid, samples were repeatedly washed with ultrapure water until neutral pH, and then they were dried at  $110^\circ C$  overnight and grounded. The bio-chars produced were denoted as AC1, AC1.5 and AC2 according to the impregnation ratio used for their preparation (1, 1.5, and 2 respectively).

### 2.3 Characterization of the activated carbon

The surface morphology of raw material and activated carbons produced from DS were observed using scanning electron microscopy (SEM) Jeol JSM 5500. Porosity of the prepared activated carbons was evaluated through N<sub>2</sub> adsorption at 77 K, using an Autosorb1-Quantachrome instrument and the NOVATouch's associated software. Prior to adsorption measurements, all samples were degassed under vacuum at 100°C for 12 hours. Adsorption equilibrium data were then analysed and fitted by using the Brunauer–Emmet and Teller (BET) and Dubinin–Radushkevich (DR) sorption models [15]. The first equation allows estimating the specific surface area ( $S_{\text{BET}}$ ) of ACs while the second provides their microporous features [15,16]. Furthermore, the pore size distribution of the active carbons was investigated using the non local density functional theory (NLDFT) based on a slit pore model [18,19]. Appropriate methods were also employed to probe additional structural parameters: for instance, mesopores volume and mesopores average size were estimated according to the Joyner and Halenda (BJH) method [8,17,18] for relative pressures  $P/P_0$  above 0.35, where  $P$  and  $P_0$  denote pressure and saturated vapour pressure of N<sub>2</sub> respectively. The total pore volume was calculated consistent with Gurvitsch rule (i.e., cumulative volume of nitrogen adsorbed to  $p/p_0 = 0.975$  corresponding to the absorbed volume plateau) [18].

In order to investigate the surface functional groups and chemical structure of the activated carbons, Fourier Transform Infrared spectra (FTIR) were recorded in the range 400-4600 cm<sup>-1</sup> using a spectrometer VERTEX 70. Dried samples were milled with IR grade KBr (Aldrich) at a mass concentration of 1% and 250 mg was used to prepare potassium bromide disk for analysis. The background spectrum of pure KBr and water vapour were subtracted from the sample spectrum.

The ability of the as-prepared AC to be used as adsorbent was examined through a model experiment designed to eliminate methylene blue (MB) dye from distilled water solution. The equilibrium of adsorption experiments were performed by adding 0.5g of AC in 100 mL of MB aqueous solutions at several concentrations ranging from 0.22mmol.L<sup>-1</sup> to 0.62 mmol.L<sup>-1</sup>. Adsorption kinetics measurements were carried out using a spectrophotometer (SPECORD 210 Plus) recording absorbance change of aqueous solutions at 665 nm corresponding to a maximum absorption wavelength of MB. The normalized MB adsorbed amount  $Q$  is calculated from the following equation:

$$Q = \frac{C_0 - C_f}{m} V \quad (1)$$

where  $C_0$  and  $C_f$  (mg / L) are respectively the initial (before adsorbent addition) and final (after adsorbent addition) concentrations of MB in solution,  $V$  (L) is the volume of the MB solution and  $m$  denotes the measured mass of AC adsorbent (g) introduced in the  $V$  volume solution.

## 3. Results and discussion

### 3.1. Yield of activated carbon

The yield of activated carbon, defined as the weight ratio of the resulting activated carbon to that of the pre-treated date stones, are determined for the three types of samples under study. The obtained values are found to vary slightly according to each sample; i.e. CA1, CA1.5 and CA2 take the values about 40%, 38.5% and 37% respectively. Comparable values are reported for the yield of AC prepared by chemical activation from olive and date stones, palm tree waste and olive tree wood [20-24]. The weight loss of precursor in general is attributed to the formation of volatile gaseous molecules like CO<sub>2</sub> and CH<sub>4</sub> accompanied by bio-oil production during pyrolysis process [25]. It is found that increasing the impregnation ratio results in an increase in the weight loss which might be explained by the higher decomposition efficiency of precursor due to higher acid concentration used in chemical treatment step.

### 3.2. FTIR analysis

Fig.1 shows the FTIR spectra of the untreated and activated carbon prepared from dates stones. It is noteworthy that the FTIR spectra of AC samples are quite similar to each other, emphasizing no significant dissimilarity

between the prepared activated carbons according to the impregnation ratio. However, some differences compared to the spectral bands of the untreated precursor can be evidenced. The FTIR spectra showed some features that are attributed to the biopolymers of the precursor. This concerns cellulose, hemicellulose and lignin components making up most of lingo-cellulosic pristine material. Indeed, the broad band in the 3000-3700  $\text{cm}^{-1}$  range of AC spectra is attributed to the stretching mode of OH in phenol group. For date stones, this peak is assigned to phenol group of lignin [26]. The two bands situated between 2800 and 3000  $\text{cm}^{-1}$  of untreated biomass are due to aliphatic CH stretching in  $\text{CH}_2$  and  $\text{CH}_3$  groups existing in cellulose structure. Those two absorption bands disappeared upon chemical activation, suggesting that cellulose structure is significantly modified through activation treatment. This behaviour is also observed through the disappearance of bands positioned between 1350 and 1450  $\text{cm}^{-1}$ , attributed to aliphatic  $\text{CH}_2$  and  $\text{CH}_3$  deformation in crystalline cellulose structure [27,28]. In untreated DS spectrum, the broad band at 1650  $\text{cm}^{-1}$  is assigned to the symmetric stretching of aromatic C=C group of lignin-phenolic groups, while the band at 1720  $\text{cm}^{-1}$  refers to the carbonyl C=O group in hemicellulose chain [29]. The absorbance of the first peak increased upon treatment and that of carbonyl group was not observed in activated carbon spectra. Band at 1155  $\text{cm}^{-1}$  is attributed to the asymmetric deformation of C-O-C of the cellulose and hemicellulose. Its absorbance is reduced in AC spectra compared to that observed in DS. The strong absorption band at 1028  $\text{cm}^{-1}$  is related to the C-OH stretching vibration of cellulose and hemicellulose [29], and its absorbance is also reduced in AC spectra. Table 1 summarizes the main differences between untreated and active DS as highlighted by FTIR spectra.

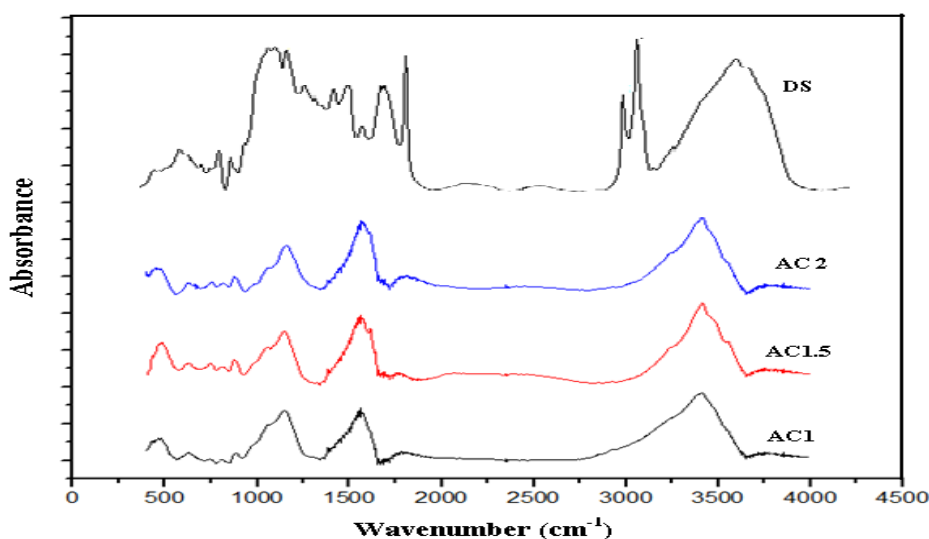


**Figure 1:** FTIR spectra of date stones and activated carbon prepared with different impregnation ratio.

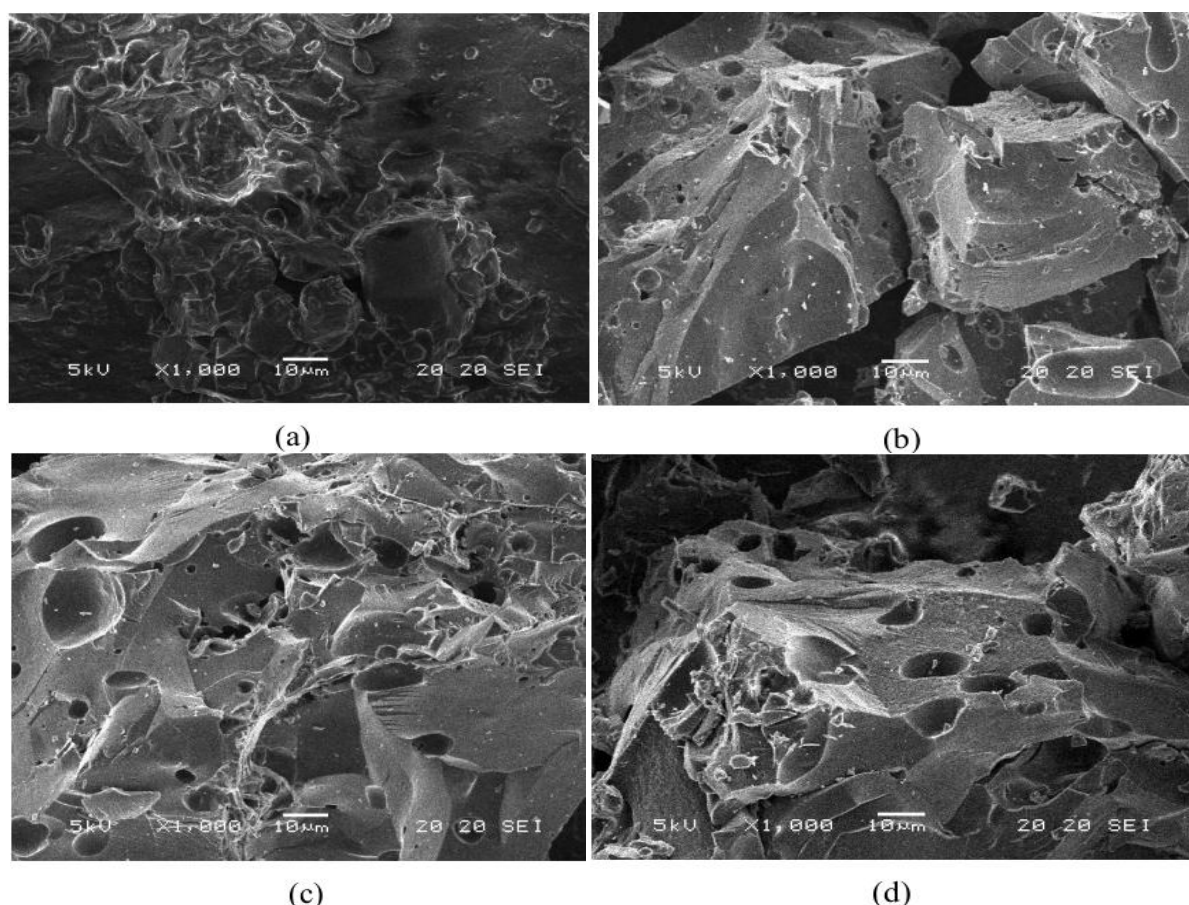
From the above discussion, the chemical activation process seems to decrease the amount of aliphatic groups of cellulose and hemicellulose, and simultaneously increases the aromaticity of material. Similar conclusion has been reported by Khan et al. [30] for a treated corncob with sulphuric acid and by Foo et al. [25] for a treated date stones by phosphoric acid. It is also reported that acid induces chemical and physical changes in precursor structure. It appears that the acid advantageously attacks the amorphous hemicellulose and lignin compounds in contrast to crystalline cellulose phase, since the impregnant diffusion in the former is expected to be easier [2,8]. Several studies reported that the acid acts as a catalyst to hydrolyse polysaccharides through protonation of the oxygen atom of glycosidic bonds in the hemicellulose and amorphous cellulose and to cleave aryl-ether linkages in the lignin structure [2,8,31]. At the end of impregnation stage, the structure of precursor particles can be viewed as small polyaromatic units connected mainly by phosphate and polyphosphate bridges. As the temperature is increased, P-O-C bonds are broken, inducing cyclization and condensation reactions that improve both aromaticity and polyaromatic unit's size. This behaviour renders the char stable around 450°C and leads to the formation of some "embryonic" graphene layers. The washing of the biomaterial transformed into AC is supposed to remove the entrapped mineral phosphate as phosphoric acid which leaves the matrix into an expanded state [8].

**Table 1:** IR Bands attribution of date stones (DS) precursor and activated carbons (AC) biochars spectra.

| DS                  |   |            | AC  |            |
|---------------------|---|------------|---|------------|
| Bands ( $cm^{-1}$ ) | Assignment  | Absorbance | Assignment  | Absorbance |
| 3000-3700           | OH stretching in phenol group of lignin                             | High       | OH stretching in phenol group                     | High       |
| 2800-3000           | Aliphatic CH stretching in $CH_2$ and $CH_3$                        | Low        |   |            |
| 1650                | Symmetric stretching of C=C groups in lignin                        | Middle     | Symmetric stretching of aromatic C=C groups       | High       |
| 1350 and 1450       | $CH_2$ and $CH_3$ deformation in crystalline structure of cellulose | High       |   |            |
| 1155                | Asymmetric deformation of C-O-C in cellulose and hemicellulose      | Middle     | Asymmetric deformation of C-O-C group             | Low        |
| 1028                | Stretching of C-OH in cellulose and hemicellulose                   | Middle     | Stretching of C-OH in cellulose and hemicellulose | Low        |

### 3.3 Structural properties

Fig 2 shows SEM analysis of both pre-treated date stones DS (a) and its corresponding bio-chars, produced at different impregnation ratios (b, c and d). Pre-treated date stones aggregates (Fig. 2 a) appear with an intact and firm structure expect for the presence of some surface-cracks resulting from grinding, according to the pretreatment procedure. Within chemical activation using phosphoric acid, biomass surface was found to rupture drastically (Fig.2 b,c,d). Indeed, when the impregnation ratio  $\chi_p$  is closed to 1, macropores with diameter ranging between 2 and 5 micrometers are formed (Fig. 2 b). As the impregnation ratio is increased, more pores having different sizes are developed (Fig 2 d). This trend becomes obvious at impregnation ratio  $\chi_p= 2$  (fig2.c).

**Figure 2:** SEM micrographs of (a) date stones and activated carbons: (b) CA 1, (c) CA 1.5 and (d) CA 2

We believe that more intricate pore network inside the AC is formed and the larger pores highlighted by SEM analysis could act as the main tributary to the smaller ones inside AC structures. To bear out this assumption, Nitrogen adsorption-desorption isotherms of the studied samples AC1 AC1.5 AC2 are presented in Figure 3. The impregnation ratio dependence on the curves recorded is clearly seen providing useful information for pores. According to the IUPAC classification [6,8], all the adsorption isotherms recorded appear as Type IV adsorption behavior which is characterized by horizontal and parallel adsorption branches over a wide range of relative pressures. In addition, it is expected that both AC1 and AC1.5 samples highlight hysteresis loops H4 and H3 in case of AC2. Those characteristics indicate that AC1 and AC1.5 samples are highly microporous materials while AC2 sample is mostly mesoporous adsorbent. Nitrogen adsorption data provides also quantitative information about the porosity of activated carbon such as total pores volume ( $V_{tot}$ ), specific surface of adsorption ( $S_{BET}$ ) and pore size distribution (PSD). Table 2 shows that all prepared samples have a large specific surface area typically in the range 721-766  $m^2/g$  with total pores volume  $V_{tot}$  varying between 0.446 and 0.704  $cm^3/g$ . The AC2 sample that is treated with  $\chi p = 2$  gives the highest  $S_{BET}$  and total pore volume resulting more probably from a creation of new pores with meso-metric sizes [33].

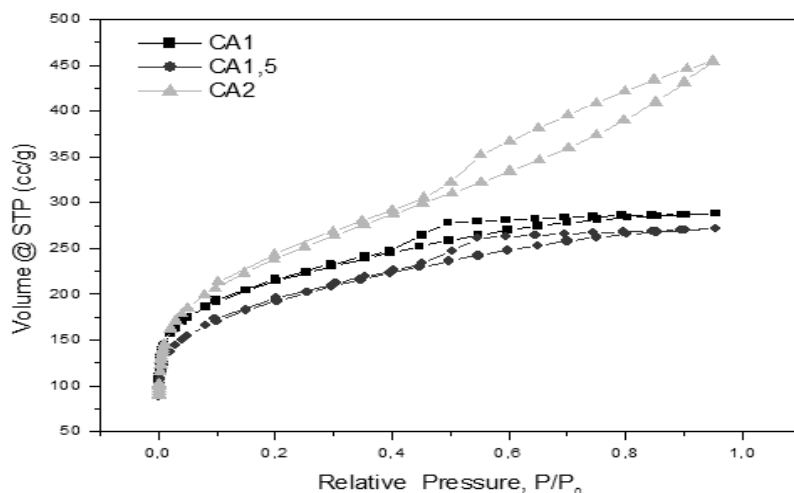


**Figure 3:**  $N_2$  adsorption–desorption isotherms at 77K of dates stones based activated carbons

Similar results have been reported assigning this effect to the amount of phosphate units and their distribution within the precursor matrix incorporated during the impregnation stage [34-36]. When the impregnation ratio value passes from 1 to 1.5, both BET surface  $S_{BET}$  and total pores volume are reduced. With this change in acid concentration, higher density of mesopores is developed as is deduced from micro-pores and meso-pores volumes contributions. This finding may accounts for the observed in  $S_{BET}$  and  $V_{tot}$ . Discrepancy between the total pore volume and the sum of both mesopore and micropore volumes is most likely due to errors in fitting, as well as assumptions in the DR model, BJH model and Gurvitsch rule.

**Table 2:** Textural characteristics of activated carbon samples.

|       | $S_{BET}$ | $V_{TOT}$ | $V_{micro}$ | $V_{micro}/V_{tot}$ | $D_{micro}$ | $V_{meso}$ | $V_{meso}/V_{tot}$ | $D_{meso}$ |
|-------|-----------|-----------|-------------|---------------------|-------------|------------|--------------------|------------|
| CA1   | 721.616   | 0.446     | 0.309       | <b>69.00%</b>       | 1.540       | 0.120      | <b>27%</b>         | 3.410      |
| CA1.5 | 639.890   | 0.420     | 0.280       | <b>66.66%</b>       | 1.612       | 0.127      | <b>30.24%</b>      | 4.303      |
| CA2   | 766.324   | 0.704     | 0.356       | <b>50.56%</b>       | 1.739       | 0.378      | <b>53.7%</b>       | 4.328      |

BET surface area ( $S_{BET}$   $m^2/g$ ), micropore surface area ( $S_{micro}$   $m^2/g$ ), total pore volume ( $V_{TOT}$ )  $cm^3/g$ , micropore volume ( $V_{micro}$ ) and mesopore volume ( $V_{meso}$ ).  $D_{micro}$ ,  $D_{meso}$  : average micropore and mesopore widths (nm).

As mentioned above, the pore size distribution can be determined using  $N_2$  desorption data coupled to the non local density functional theory (NLDFT). The NLDFT, based on a slit pore model, leads to reliable pore size distribution over the complete range of micro- and mesopores [19,37]. The calculated distributions are plotted in Figure 4 for three studied samples showing a wide distributions ranging from micro- to mesopores. More

interestingly, it is found that the increase of the impregnation ratio shifts the peak of distribution to higher pore widths as it is reported in Table 2.

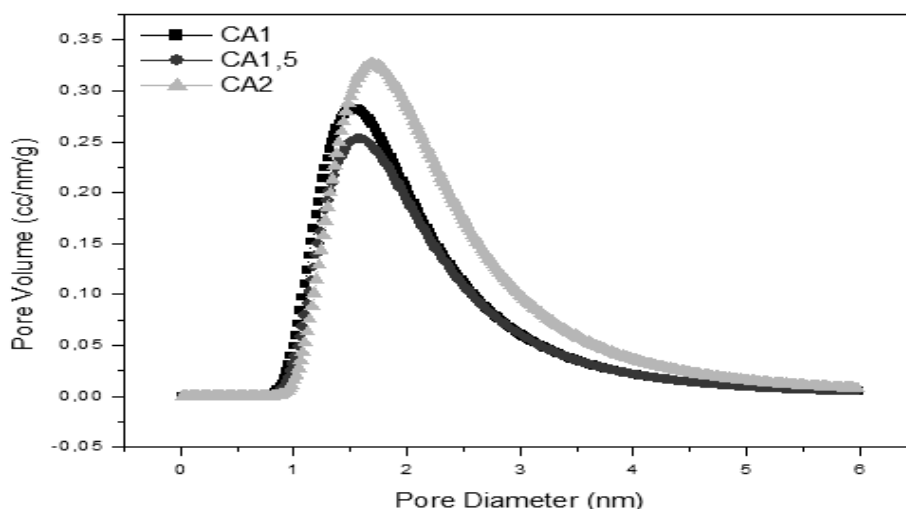


**Figure 4:** Pore size distribution of AC samples

### 3.4 Methylene Bleu adsorption on AC

Methylene Bleu batch-adsorption was performed at 30°C using AC2 sample derived from date stones. The effect of the inlet MB concentration on adsorption was investigated. As shown in Fig. 5, the uptake capacity  $Q$  of the adsorbent AC2 increases up to 21mg/g by increasing the MB concentration from 0.22 to 0.62mmol.L<sup>-1</sup>. This result was expected because increasing of the adsorbate initial concentration enhances the driving force of the concentration gradient in order to overcome the mass transfer resistance of the adsorbate between the aqueous and solid phases [1]. Moreover, as the adsorbate concentration increases, the number of collisions between the adsorbate molecules and the adsorbent functional groups is also amplified and could leading to an enhancement of the adsorption capacity [38].

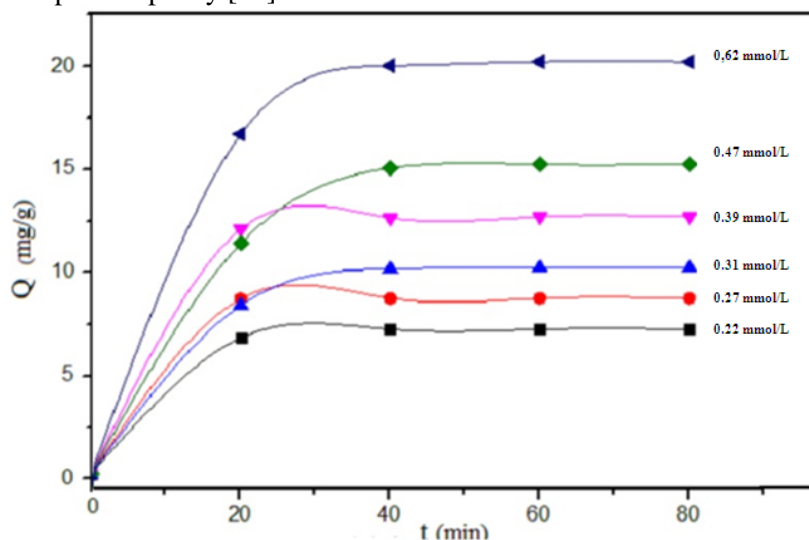


**Figure 5:** Adsorption kinetic of methylene blue on AC2.

In order to correlate the amount of adsorbate uptake at equilibrium  $Q_e$  by AC2 sample and its equilibrium concentration in the solution  $C_e$ , two equilibrium models namely, Langmuir and Freundlich were tested to fit experimental sorption isotherm of MB. The former model assumes that the adsorption takes place at homogeneous sites with uniform energy levels while the second describes the heterogeneous systems with non-identical adsorption sites. We use here only the logarithmic form of Freundlich equation because the equilibrium experiment data fitted Freundlich isotherm equation better than Langmuir isotherm, especially at high BM concentrations. The equation is given by the relationship [39]:

$$\ln Q_e = \ln K + \frac{1}{n} \ln C_e \quad (2)$$

$C_e$  (mg/g (L/mg)<sup>1/n</sup>),  $Q_e$  (mg/g) are respectively equilibrium concentration of adsorbate and amount adsorbed at equilibrium.  $K$  is roughly an indicator of the adsorption capacity and  $1/n$  is the adsorption intensity. In general, as the  $K$  value increases, the adsorption capacity of adsorbent for a given adsorbate increases, whereas the magnitude of the exponent  $1/n$ , gives an indication of the favorability of adsorption [39]. The Freundlich parameters  $K_F$  and  $1/n$  are calculated from the slope and intercept of the isotherms and are given in Fig.6.

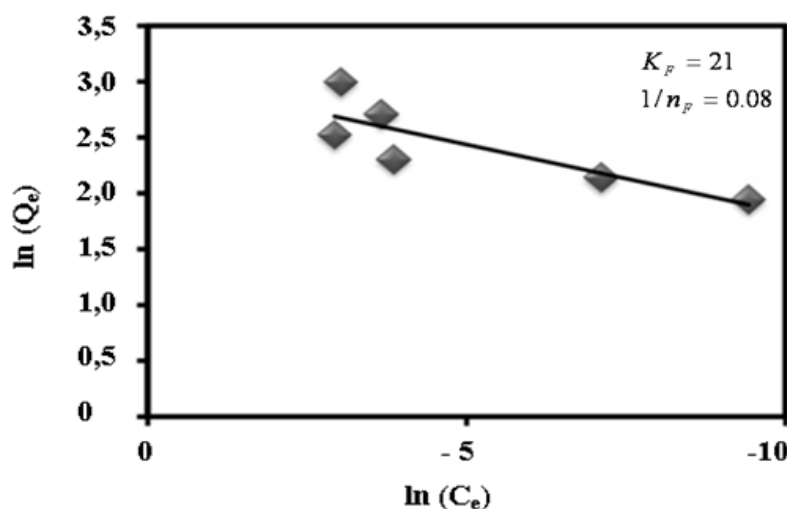


**Figure 6:** Simulation of the adsorption isotherm of MB on AC2 by Freundlich model

The value of  $1/n$  is less than 1 indicates favorable adsorption condition for the removal of BM on the activated carbon AC2. According to Freundlich model assumptions, AC2 sample would have a high heterogeneous adsorption sites. This possible feature could be assigned to the broad pore size distribution and especially to different chemical functional groups within AC2 and their interactions with the cationic dye BM.

## Conclusion

In this work, activated carbons were produced from date stones agriculture by-products by chemical activation and using various impregnation  $H_3PO_4$  concentrations. The samples were characterized by FTIR spectroscopy, it was demonstrated that chemical activation reduced aliphatic groups of the biomaterial and increased its aromaticity. Structural characterization conducted by SEM and  $N_2$  adsorption-desorption revealed that a highly porous AC were synthesized. Furthermore, as impregnation ratio of  $H_3PO_4$  is increased, pore volumes and BET specific surface of AC is enhanced. It induces a shift of pore size distribution from micropore to mesopore region by increasing the mesoporosity of AC. The AC2's surface area (766 m<sup>2</sup>/g), total pore volume (0.7cm<sup>3</sup>/g) and ratio of mesopore to total pore volume (0.537) revealed that the AC2 can be considered as a promising adsorbent for removal of different pollutants from water. Therefore, the adsorption performance and capacity of the AC2 for removal of MB from aqueous solution were investigated by measuring adsorption kinetics and isotherm. Results indicate that adsorption capacity of AC was considerably affected by initial concentrations and according to experimental conditions, the highest adsorption capacity  $Q_e$  was found to be 21mg/g. The adsorption isotherm was fitted by Freundlich model which gives a better fit of experimental data, indicating that AC2 contains high heterogeneous adsorption sites.

From the overall results, date stones can be a promising biomaterial candidate as precursor for AC preparation. It would be more effective in waste water treatment by optimizing conditions of its chemical activation and it is expected to be used in other applications like anode material for sodium batteries.

**Acknowledgments-**The authors would like to thank the Center of Analysis and Characterization of Cadi Ayyad University for their support for this research.



## References

1. Hadi P., Xu M., Ning C., Lin C-S-K., G. McKay, *Chem. Eng. J.* 260 (2015) 895.
2. Pandey S., Negi, P., Binod, C., Larroche, Lingocellulosic Biomass in Pretreatment of biomass process and technologies, ed., Elsevier. (2015) 3.
3. Heidler J., R.U. Halden, *Environ. Sci. Technol.* 42 (2008) 6324.
4. Heibati B., S. Rodriguez-Couto, M. A. Al-Ghouti, M. Asif, I. Tyagi, S. Agarwal, V.K. Gupta, *J. Mol. Liq.* 208 (2015) 99.
5. Hall J., Ecological and economical balance for sludge management options, in: Proc. Work. Probl. Around Sludge. (1999) 155.
6. Bouchelta C., M.S. Medjran, O. Bertrand, J. Bellat, *J. Anal. App. Pyr.* 28 (2008) 70.
7. Hameed B.H., J.M. Salman, A.L. Ahmad, *J. Hazard. Mater.* 163 (2009) 121.
8. Marsh H., F.R. Reinoso, Activated carbon, Science & Technology Books, ed., Elsevier, (2006) 47.
9. Royer B., N.F. Cardoso, E.C. Lima, J.C.P. Vagheti, R.C. Veses, *J. Hazard. Mater.* 164 (2009) 1213.
10. Yang J., K. Qiu, *Chem.Eng.J.* 165 (2010) 209 –217.
11. Senthilkumar S., P.R. Varadarajan, K. Porkodi, C.V. Subbhuraam, *J. Colloid. Interface. Sci.* 284 (2005) 78.
12. Ahmed M.J., S.K. Theydan, *Fluid. Phase. Equilib.* 317 (2012) 9.
13. Theydan S.K., M.J. Ahmed, *Powder. Technol.* 224 (2012) 101.
14. Hared A., Thèse de l'Ecole des Mines d'Albi-Carmaux-France. (2007) 53.
15. Brunauer S., P.H. Emmett, E. Teller, *J. Am. Chem. Soc.* 60 (1938) 309.
16. Foo K.Y., B. H. Hameed, *Chem. Eng. J.* 156 (2010) 2.
17. Sing K. S.W., R. T. Williams, *Ads. Sci. Techn.* 22 (2004) 773.
18. Lowell S., J.E. Shields, M.A. Thomas, M. Thommes, Characterization of porous solids and powders: surface area, pore size and density, ed., Springer Netherlands.(2004)
19. Do D.D., Do H.D., *Ads. Sci. Tech.* 21 (2003)
20. Chouchene, Thèse de l'Ecole Nationale d'Ingénieurs de Monastir-Tunisie et de l'Université de Haute-Alsace France. (2010)
21. Z. Belala, M. Jeguirim, M. Belhachemi, F. Addoun, G. Trouvé, *Desalination.* 271 (2011) 80.
22. Ould-Idriss, M. Stitou, E.M. Cuerda-Correa, C. Fernández-González, A. Macías-García, M.F. Alexandre-Franco, V. Gómez-Serrano, *Fuel. Process, Techn.* 92 (2011) 261.
23. Baccar R., J. Bouzid, M.Feki, A. Montiel, *J. Hazard. Mater.* 162 (2009) 1522.
24. Kurniawan, S. Ismadji, *J. Taiwan. Instit. Chemic. Eng.* 42 (2011) 826.
25. Babiker M. E., A. R. Aziz, M. Heikal, S. Yusup, M. Abakar, *Intern. J. Env. Sci. Dev.* 4 (2013) 521.
26. Pereira S. C., L. Maehara, C.M.M. Machado, C.S. Farinas, *Renew. Energ.* 87 (2016) 607.
27. Müller G., C. Schöpfer, H. Vos, A. Kharazipour, A. Polle, *BioResources.* 4 (2009) 49.
28. Popescu C.M., M.C. Popescu, G. Singurel, C. Vasile, D.S. Argyropoulos, S. Willfor, *Appl. Spectr.* 61 (2007) 1168.
29. Traoré M., J. Kaal, A. M. Cortizas, *Spectr. Acta. A: Molecul. Biomolecul. Spectr.* 153 (2016) 63.
30. Khan N. M., F. M. Wahab, *J. Hazard. Mater.* 141 (2007) 237.
31. Pandey M. P., C. S. Kim, *Chem. Eng. Technol.* 34 (2011) 29.
32. Newalkar G., K. Iisa, A. D. D'Amico, C. Sievers, P. Agrawal, *Energ. Fuel.* 28 (2014) 5144.
33. Sánchez- Aznar J., Thesis in School of Chemical Science and Engineering, Sweden. (2011)
34. Guo Y., D.A. Rockstraw, *Bioresour. Technol.* 98 (2007)1513.
35. Baquero M.C., L. Giraldo, J.C. Moreno, F. Suárez-García, A. Martínez-Alonso, J.M.D.Tascón, *J. Anal. Appl. Pyrolysis.* 70 (2003) 779.
36. Macias-Garcia M.A. Diaz-Diez V. Gomez-Serrano M.C. Gonzalez, *Smart Mater. Struct.* 12 (2003) N24.
37. Balbuena P.B., Gubbins KE., *Langmuir.* 9 (1993) 1801.
38. Aksu Z., Akın A.B., *Chem. Eng. J.* 165 (2010) 184.
39. Freundlich H. M. F., *J. Phy. Chem.* 57 (1906) 385.

(2017) ; <http://www.jmaterenvironsci.com>